The Journal of Clinical Pharmacology
2022, 62(3) 422–433

DOI: 10.1002/jcph.1974

Population Pharmacokinetics of TAK-931, a Cell Division Cycle 7 Kinase Inhibitor, in Patients With Advanced Solid Tumors

Xiaofei Zhou, PhD[1], Aziz Ouerdani, PhD[2], Paul Matthias Diderichsen, PhD[3], and Neeraj Gupta, PhD, FCP[1]

Abstract

A population pharmacokinetic (PK) analysis was conducted to characterize sources of interpatient variability on the PK of TAK-931, a cell division cycle 7 kinase inhibitor, in adult patients with advanced solid tumors using data from 198 patients who received oral TAK-931 over the range of 30 to 150 mg once daily in multiple dosing schedules in 2 phase 1 and 1 phase 2 clinical studies. A 2-compartment model with 2 transit compartments describing the absorption and first-order linear elimination adequately described the PK of TAK-931. The apparent oral clearance (CL/F) of TAK-931 was estimated to be 38 L/h, and the terminal half-life was estimated to be approximately 6 hours. Creatinine clearance (CrCL) was identified as a covariate on CL/F, and body weight as a covariate on CL/F, apparent central volume of distribution, and apparent intercompartmental clearance. Simulations using the final model indicated that the effect of CrCL (≥35 mL/min) or body weight (29.8-127 kg) on TAK-931 systemic exposures was not considered clinically meaningful, suggesting that no dose adjustments were necessary to account for body weight or renal function (CrCL ≥35 mL/min). Sex, age (36-88 years), race, and mild hepatic impairment had no impact on the CL/F of TAK-931. Taken together, the population PK analysis supports the same starting dose of TAK-931 in Asian and Western cancer patients in a global setting.

Keywords

advanced solid tumors, CDC7, global, pharmacokinetics, race

Cell division cycle 7 (CDC7) kinase is a serine/threonine kinase highly expressed in various types of cancer (eg, ovarian, breast, colorectal, and lung)[1,2] and correlated with poor prognosis.[3–5] It is involved in the DNA damage response[6,7] as well as DNA replication,[8,9] suggesting that CDC7 plays important roles in both cell proliferation during the S phase and genomic stability in the DNA damage response.[10] CDC7 appears to be a critical gene for the proliferation and survival of cancer cells, and inhibition of CDC7 is expected to be antiproliferative and induce apoptosis in a broad range of cancers.[11]

TAK-931, 2-[(2S)-1-azabicyclo[2.2.2]oct-2-yl]-6-(3-methyl-1H-pyrazol-4-yl)thieno[3,2-d]pyrimidin-4(3H)-one hemihydrate (the chemical structure presented in Figure S1), is a small molecule that inhibits CDC7 kinase and is currently under development for the treatment of patients with advanced malignancies.[12–15] An open-label, dose-escalation, first-in-human study in adult patients with advanced nonhematologic tumors was conducted in Japan, and various dosing schedules were evaluated (NCT02699749).[13,16] TAK-931 administered at 50 mg daily for 14 days in a 21-day treatment cycle was investigated in an open-label, phase 2 study in adult patients with metastatic pancreatic, colorectal, and other advanced solid tumors in the United States with a safety lead-in cohort to confirm comparable exposures and safety profiles between Asian and Western patients (NCT03261947).[15] Clinical development was subsequently transitioned from a capsule to a tablet formulation. The relative bioavailability of tablets in reference to capsules was assessed.[14]

[1]Millennium Pharmaceuticals, Inc., Cambridge, MA, USA, a wholly owned subsidiary of Takeda Pharmaceutical Company Limited, Cambridge, Massachusetts, USA
[2]Certara, Data Science Services, Paris, France
[3]Certara, Data Science Services, Breda, The Netherlands

Submitted for publication 21 May 2021; accepted 21 September 2021.

Corresponding Author:
Neeraj Gupta, PhD, FCP, Quantitative Clinical Pharmacology, Millennium Pharmaceuticals, Inc., Cambridge, MA, USA, a wholly owned subsidiary of Takeda Pharmaceutical Company Limited, 40 Landsdowne Street, Cambridge, MA 02139
Email: neeraj.gupta@takeda.com

Authors who are Fellows of the American College of Clinical Pharmacology: Neeraj Gupta.

Table 1. Clinical Studies Included in the Population PK Analysis

Study (Phase, Type) and Clinical Trials.gov Identifier	Patient Population	N	Regimen	TAK-931 Dose	PK Sampling Schedule
TAK-931-1002 (Phase 1) NCT02699749	Adult patients with advanced nonhematologic tumors	80	*Schedule A*: PIC once daily 14 days on/7 days off; 21-day cycle	*Schedule A*: 30, 40, 50, 60 mg	*Schedule A*: Day 1 and day 8 of cycle 1: before dosing and 0.5, 1, 2, 4, 6, 8, 12, and 24 h after dosing
			Schedule B: PIC once daily 7 days on/7 days off; 28-day cycle	*Schedule B*: 60, 80, 100, 120 mg	*Schedule B*: Day 1 and day 7 of cycle 1: before dosing and 0.5, 1, 2, 4, 6, 8, 12, and 24 h after dosing
			Schedule D: PIC once daily 21 days; 21-day cycle	*Schedule D*: 20, 30, 40 mg	*Schedule D*: Day 1 and day 8 of cycle 1: before dosing and 0.5, 1, 2, 4, 6, 8, 12, and 24 h after dosing
			Schedule E: PIC 2 days on/5 days off; 21-day cycle	*Schedule E*: 100, 120, 150 mg	*Schedule E*: Day 1 and day 9 of cycle 1: before dosing and 0.5, 1, 2, 4, 6, 8, 12, and 24 h after dosing
TAK-931-1003 (Phase 1, relative bioavailability) NCT03708211	Adult patients with metastatic pancreatic cancer, metastatic colorectal cancer, and other advanced solid tumors	20	**Sequence 1**: 80 mg PIC at day 1 followed by 80-mg tablet at day 3 **Sequence 2**: 80-mg tablet at day 1 followed by 80-mg PIC at day 3	80 mg	Before dosing and 0.5, 1, 2, 4, 6, 8, 24, and 48 h after dosing
TAK-931-2001 (Phase 2, safety and efficacy) NCT03261947	Adult patients with advanced nonhematologic tumors	98	50 mg PIC once daily 14 days on/7 days off; 21-day cycle	50 mg	*Intensive sampling for safety and disease-specific cohorts*: Day 1 and day 8 of cycle 1: before dosing and 0.5, 1, 2, 4, 6, 8, and 24 h after dosing *Sparse sampling for disease-specific cohorts*: Cycle 1 day 1: before dosing and 1, 2, and 4 hours after dosing Cycle 1 day 8, cycle 2 day 1 and cycle 2 day 8: before dosing and 2 h after dosing

PIC, powder-in-capsule; PK, pharmacokinetic.

The objectives of this analysis were to develop a population pharmacokinetic (PK) model of TAK-931 and quantify the impact of the sources of PK variability in adult cancer patients.

Methods

Clinical Studies

All studies were conducted in accordance with the protocol; the ethical principles with origins in the Declaration of Helsinki; the informed consent regulations stated in Title 21 CFR, Part 20, in accordance with the International Council for Harmonization Good Clinical Practice (E6) §4.8,[17] and all applicable local regulations. The protocol, its amendments, and the patient informed consent forms were reviewed by the institutional review boards and independent ethics committees of the participating study sites. All patients provided written informed consent for participation in the study.

A summary of the studies included in the population PK analyses is provided in Table 1. The analysis data set included all patients who received TAK-931 and had at least 1 quantifiable postdose TAK-931 plasma concentration.

Analytical Methods

TAK-931 plasma samples were analyzed by a validated, solid-phase, extraction liquid chromatography–tandem mass spectrometry method. The dynamic range was

0.5 to 1000 ng/mL. The assay precision for the quality control samples (1.5-750 ng/mL) ranged from 4.7%-8.9%, and accuracy (% bias) ranged from –9.6% to 5.3%.

Pharmacokinetic Analyses

The analysis was performed using nonlinear mixed-effects modeling implemented in NONMEM version 7.3.0 (ICON, Hanover, Maryland). Graphical analysis and simulations were performed using R version 3.6.3 (R Foundation for Statistical Computing, Vienna, Austria).

Structural and Statistical Model Development. All analyses were performed using the first-order conditional estimation method of NONMEM with interaction and considered log-transformed TAK-931 plasma concentration data ("log-transform both sides"[18]). Interindividual variability (IIV) in the PK parameters was modeled assuming a log-normal distribution:

$$\theta_{ki} = \theta_k \times e^{\eta_{ki}} \quad (1)$$

where θ_{ki} denotes the individual value of parameter k for the ith patient, θ_k denotes the population typical parameter value, and η_{ki} denotes the interindividual random effect for the ith patient, assumed to have mean of 0 and variance $\omega_k{}^2$. An additive residual error of the log-transformed concentration data (equivalent to an exponential residual error on the untransformed scale) was used:

$$\log\left(Y_{ij}\right) = \log(C_{ij}) + \varepsilon_{ij} \quad (2)$$

where Y_{ij} is the jth observed concentration for the ith patient, C_{ij} is the corresponding predicted concentration, and ε_{ij} is the additive residual error under the assumption that $\varepsilon \sim N(0, \sigma^2)$.

The PK profiles of TAK-931 were first described with a 1-compartment model of disposition with first-order linear elimination and first-order absorption rate (k_a). Two- and 3-compartment models of disposition were also investigated. First- and zero-order absorption processes were considered, with k_a associated with and without lag time and delays described by 1, 2, or 3 transit compartments. IIV was evaluated in a stepwise fashion. The final model-building step consisted of a covariate evaluation based on a stepwise covariate modeling (SCM) procedure.

Covariate Model Development. Covariate model development was performed in 2 steps. Initially, a univariate covariate screening identified covariates on PK parameters with IIV that were significant at the $\alpha = .01$ level. In addition, body weight was evaluated as a covariate on all model parameters to allow the model to estimate allometric effects on TAK-931 PK. Subsequently, parameter-covariate relationships identified as statistically significant based on univariate analysis were evaluated and tested for significance in a multivariate SCM procedure, as implemented in Perl-speaks-NONMEM.[19] Statistical significance was assessed at $\alpha = .05$ and $\alpha = .001$ significance levels during forward inclusion and backward exclusion, respectively.

Demographic covariates (baseline age, body surface area, body mass index, body weight, sex, and race), baseline laboratory tests (bilirubin [BILI] and creatinine clearance [CrCL]), hepatic impairment status (normal hepatic function: total BILI and aspartate aminotransferase [AST] $\leq$ upper limit of normal [ULN]; mild hepatic impairment: total BILI $\leq$ ULN and AST $>$ ULN, or ULN $<$ total BILI $\leq 1.5 \times$ ULN and AST of any value), and Eastern Cooperative Oncology Group status were evaluated during the univariate screening.

CrCL was derived from serum creatinine according to the Cockcroft-Gault equation[20]:

$$CrCL\left(\frac{mL}{min}\right) = \left(\frac{(140 - Age\ (years)) * Weight\ (kg)}{72 * Serum\ creatinine\ \left(\frac{mg}{dL}\right)}\right) * \begin{cases} 1, & if\ male \\ 0.85, & if\ female \end{cases} \quad (3)$$

Continuous covariates were incorporated into the population model by a power model centered on the median value of the covariate, shown in Equation 4:

$$P_{ki} = \theta_k \times \left(\frac{X_{ij}}{M\left(X_j\right)}\right)^{\theta_j} \quad (4)$$

where P_{ki} is the typical estimate of the parameter k for patient i, X_{ij} is the value of continuous covariate X_j for patient i, $M(X_j)$ is the median value of covariate X_j in the analysis data set, θ_k is the population typical value of the parameter k, and θ_j is a coefficient that reflects the effect of covariate X_j on the parameter.

Categorical covariates were incorporated into the population model using a proportional structure, with the most common level of the covariate being the reference and the other values of the covariate being expressed relative to that reference:

$$P_{ki} = \theta_k \times \left(1 + \theta_j\right)^{X_{ij}} \quad (5)$$

where P_{ki}, θ_k, and θ_j are as defined for continuous covariates, and X_{ij} is an indicator variable for patient i for categorical covariate X_j with value 1 for the nonreference category and 0 for the reference category.

Model selection was based on the change in minimum value of the objective function value (OFV). In

addition, a clinically relevant change in parameter value across the 5th to 95th percentiles of the covariate values obtained from patients in the analysis data set and a reduction in the associated IIV of at least 10% of the variance,[21,22] upon inclusion of the proposed covariate, were required to justify the retention of statistically significant covariates identified during the SCM in the final model.

Final Model Evaluation. Evaluation of the final model was based on a selection of statistical and graphical diagnostics.[23,24] A nonparametric bootstrap procedure was performed to evaluate the stability of the final model and to obtain nonparametric confidence intervals (CIs).[25] The bootstrap analysis was performed by creating 1000 replicates of the data set, obtained by random resampling of patients from the original data set, with replacement. The final model was then repeatedly fitted to each of the replicated data sets, and CIs were subsequently obtained based on the distribution of parameter estimates from the bootstrap runs. Specifically, the median and 95%CIs were defined as the 50th, 2.5th, and 97.5th percentiles of the results obtained from the individual bootstrap runs. Bootstrap statistics were based on replicates that converged successfully.

Prediction-corrected visual predictive checks (pcVPCs) were created to evaluate the predictive performance of the model.[26,27] Plots of the observed data distribution were compared with simulated distributions from 1000 replicates of the PK data set obtained using the final PK model. Specifically, the median and 2.5th and 97.5th percentiles of the observed data were contrasted with the 95%CIs of each of these percentiles obtained from the simulations. The pcVPCs were also presented following stratification by representative categorizations of covariates that were included in the final model.

Model-Based Simulations

Simulations were performed to evaluate the effect of renal impairment on steady-state exposures of TAK-931. CrCL was simulated for 1000 patients in each of the required categories of renal function (moderate renal impairment, 30 mL/min $\leq$ CrCL $<$ 60 mL/min; mild renal impairment, 60 mL/min $\leq$ CrCL $<$ 90 mL/min; normal renal function, CrCL $\geq$ 90 mL/min). CrCL was sampled from a uniform distribution bounded by the limits of the CrCL required for each group. Subsequently, apparent oral clearance (CL/F) was derived from the simulated CrCL in each of these virtual patients (also including the effect of unexplained IIV in CL/F), and steady-state area under the plasma concentration–time curve (AUC) was then obtained, following a nominal dose of 50-mg daily dose, according to Equation 6:

$$AUC = \frac{Dose}{CL/F} \tag{6}$$

The resulting AUC was normalized to the AUC obtained from the typical (reference) patient, with a CrCL of 90.45 mL/min (median value). Subsequently, the median and 5th and 95th percentiles of the normalized AUC were obtained in each renal function category to summarize the typical study, as educated by the final model parameters. The impact of uncertainty of the final model parameter estimates was derived by repeating the simulation 1000 times on the basis of parameter estimates obtained from each of the individual bootstrap replicates. The 90%CI (defined as the 5th–95th percentile range of the normalized AUC obtained in each of the individual study replicates) was then derived.

The same procedure was followed to simulate the impact of body weight.

Results

Summary of Analysis Data Set

The population PK analysis included data from 198 patients who contributed 2678 postdose plasma concentrations. A total of 55 postdose concentrations were below the limit of quantification, constituting a small percentage (2%) of the available postdose concentration data. As a result, concentrations that were below the limit of quantification were excluded during the population PK analysis. The 198 patients included in the population PK analysis each contributed a median of 16 plasma concentrations to the analysis (range, 1-21).

Key demographics and baseline characteristics of all patients included in the analysis, stratified by clinical study, are summarized in Table 2.

Base Model Development

The initial model development considered linear models with first-order elimination and first-order k_a. One-, 2-, and 3-compartment models of disposition were evaluated, and the 2-compartment model was selected. The absorption process was best described with 2-transit compartments (OFV reduction by 171 points). Different numbers of integer transit compartments for absorption were evaluated. The model with 2 transit compartments resulted in an adequate fit to the observed data (Table S1). As such, models estimating noninteger numbers of transit compartments[28] were not considered. A simplification of the model, where k_a = transit rate constant, was performed and led to a nonsignificant (at the $\alpha = .05$ level) increase of the

Table 2. Summary of Demographic and Baseline Characteristics of All Patients (N = 198) Included in the Population PK Analysis

Baseline Characteristic	Median (Range) or Categories (%)
Continuous	
Age, y	61 (36-88)
Body weight, kg	65.8 (29.8-127)
Body surface area, m^2	1.74 (1.11-2.43)
CrCL, mL/min	89.9 (35-204)
Bilirubin, μM	8.6 (1.7-24.5)
Categorical	
Race	
Asian	55.1
White	33.3
Black or African American	4
Other	7.6
Sex	
Female	60
Male	40
Age	
<75 years old	91.4
≥75 years old	8.6
Renal function	
Normal	50.5
Mild renal impairment	32.8
Moderate renal impairment	17.7
Hepatic function	
Normal	80.3
Mild hepatic impairment	19.7
Baseline Eastern Cooperative Oncology Group performance	
0	55.6
1	44.4

AST, aspartate aminotransferase; CrCL, creatinine clearance; SD, standard deviation; TB, total bilirubin; ULN, upper limit of normal.
Normal hepatic function, TB and AST ≤ ULN; mild hepatic impairment, TB ≤ ULN and AST > ULN or TB > 1 to 1.5 × ULN and AST of any value.
Normal renal function, CrCL ≥ 90 mL/min; mild renal impairment, CrCL of 60-89 mL/min; moderate renal impairment, CrCL of 30-59 mL/min.

OFV (0.7 points). Hence, the model was parameterized in terms of clearances and volumes and included the following parameters: CL/F, apparent central volume of distribution (V_c/F), apparent peripheral compartment volume, apparent intercompartmental clearance (Q/F), and transit rate constant. IIV on the mean transit time (MTT) was retained during the first round of the IIV investigation (OFV drop by 716 points) followed by a second round, where IIV on clearance was retained (OFV reduction by 589 points).

Covariate Model Development

The effects of covariates of interest (including body weight, age, BILI, CrCL, sex, race, and normal or mild hepatic impairment) were evaluated. Race was evaluated as White vs Asian vs others.

Visual inspection of exploratory scatterplots of individual patient empirical Bayes estimates and continuous covariates indicated a potential relationship between age, CrCL, and body size–related covariates (body weight, body surface area, and body mass index) and CL/F (not shown). SCM procedures identified CrCL as a statistically significant covariate of CL/F, suggesting that CrCL is a robust predictor of clearance. Body weight was identified as a statistically significant covariate of CL/F, V_c/F, and Q/F.

The covariate-parameter relationships retained in the final model are presented in Equation 7:

$$\begin{aligned} \text{CL/F (L/hr)} &= 38 \times \left(\frac{\text{CrCL}}{90.45\ mL/min}\right)^{0.325} \times \left(\frac{\text{BW}}{65.95\ kg}\right)^{0.484} \\ V_c/\text{F (L)} &= 194 \times \left(\frac{\text{BW}}{65.95\ kg}\right)^{0.867} \\ Q/\text{F (L/hr)} &= 7.71 \times \left(\frac{\text{BW}}{65.95\ kg}\right)^{0.938} \end{aligned} \quad (7)$$

Specifically, race, sex, Eastern Cooperative Oncology Group status, and hepatic function were not identified as covariates on CL/F, and none of the evaluated covariates were statistically significant predictors of MTT in the SCM. Figure 1 indicated the lack of impact of race, sex, and hepatic function on TAK-931 CL/F. A trend was observed between CL/F and race, and between CL/F and sex. This could be explained by the correlation between the 2 covariates and body weight. This was confirmed by the lack of trend in the random effects (Figure 2).

Final Model

A scheme of the final model is displayed in Figure S1. Goodness-of-fit diagnostic plots for the final model are presented in Figure S2, demonstrating that the model described the data with no obvious bias in residual error with respect to either time or concentration. A non-diagonal OMEGA matrix estimating the correlation between CL/F and apparent volume of distribution was evaluated. Since pcVPC plots showed good agreement between the observed and model-predicted concentrations in the first 30 hours (Figure 3), during the full time range (Figure S3) and during the absorption phase (Figure S4), other correlations were not explored. Similarly, good agreement between the observed and model-predicted concentrations was noted when stratified by covariates included in the final population PK model (Figure 3B/C and Figure S3B/C). The model development history and selection are provided in Table S1.

A high percentage (94.9%) of the bootstrap analyses converged successfully, confirming the final model's robustness. The parameter estimates obtained from the final model were similar to the median parameter values obtained from the bootstrap analyses, confirming that the final parameter estimates

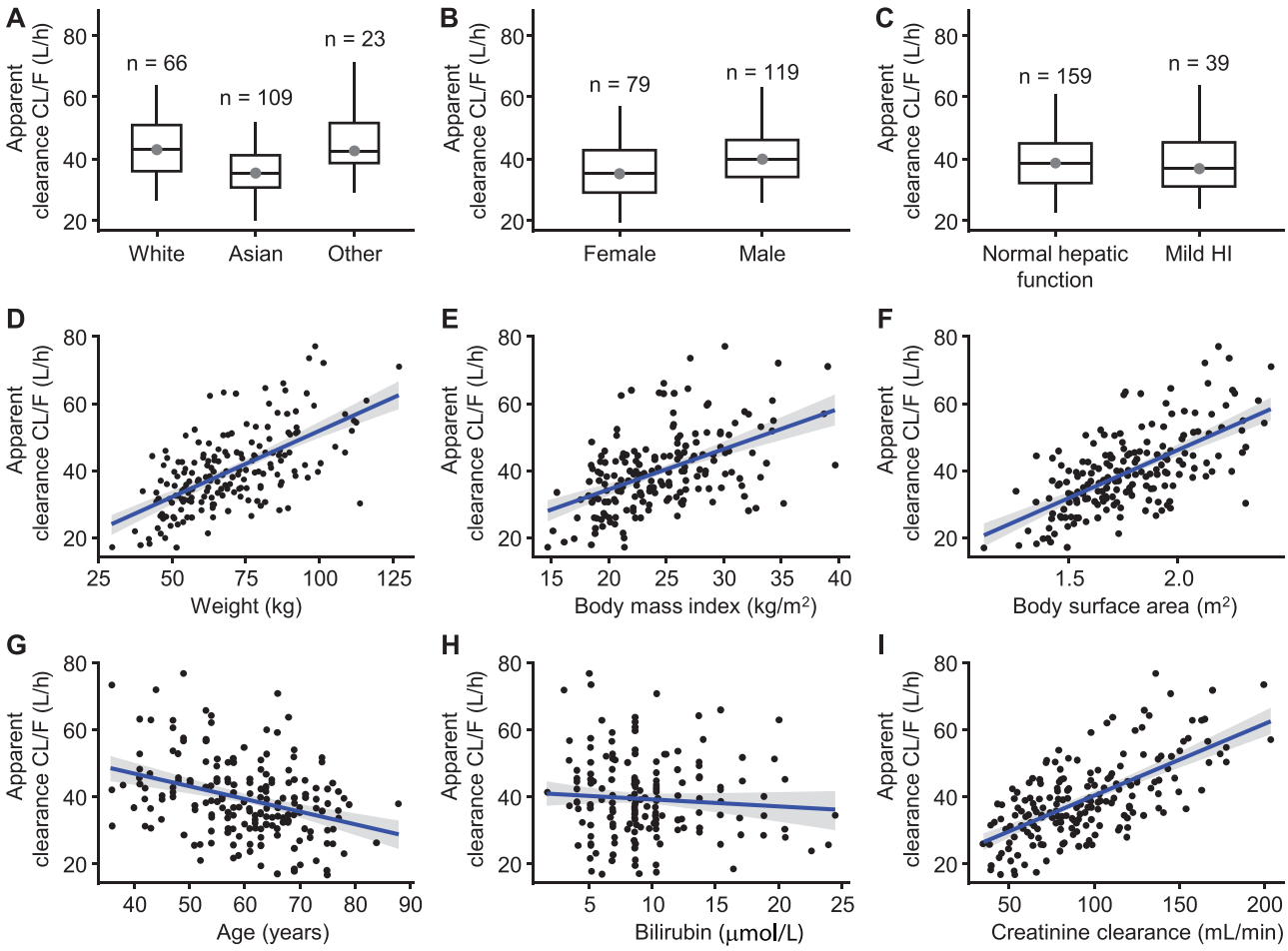

Figure 1. Relationship between covariates and TAK-931 CL/F. Panels A–C box plots: horizontal lines comprising the box are the 25th, 50th (median), and 75th percentiles. The whisker ends denote 1.5 times the difference between the 25th and 75th percentiles. Panels D–I: black closed circles are the individual estimates of TAK-931 apparent clearance; the blue lines show linear regressions, and gray shades are the corresponding 95% confidence intervals of linear regressions. CL/F, apparent oral clearance; HI, hepatic impairment.

corresponded to a global maximum likelihood estimate (Table 3).

The relationship between CrCL and CL/F was implemented using a nonlinear power function. A 10% increase in CrCL and body weight was predicted to result in a 3% (95%CI, 2-4) and 5% (95%CI, 3-7) increase in CL/F, respectively. The variance of the unexplained IIV on CL/F increased by 18% and 22% when body weight and CrCL, respectively, were eliminated from the final model, justifying the retention of both relationships in the model.

Model-Based Simulations

The simulated TAK-931 concentration-time course after daily administration of 50 mg of TAK-931 during 14 days is presented in Figure 4. This dose regimen has been investigated in a phase 2 study of TAK-931 in patients with metastatic pancreatic cancer, metastatic colorectal cancer, and other advanced solid tumors. Corresponding summary statistics of AUC, average concentration, maximum concentration, and minimum concentration, predicted on days 1 and 14, are tabulated in Table S2. Steady state was reached quickly after ≈3 days of multiple dose administrations. Between days 1 and 14, the median AUC, average concentration, maximum concentration, and minimum concentration increased by 11%, 11%, 6%, and 44%, respectively.

A forest plot (Figure 5) demonstrates the effect of renal function (Figure 5A) and body weight (Figure 5B) on steady-state exposure to TAK-931.

It shows that the largest increase in AUC was observed in patients with moderate renal impairment. Normalized AUC (corresponding to a typical patient with median CrCL and body weight [90.45 mL/min and 65.95 kg, respectively] and no unexplained IIV) increased with decreasing renal function. The median normalized AUC (90%CI, reflecting parameter uncertainty) was 0.91 (0.889-0.929), 1.06 (1.04-1.07), and 1.25 (1.19-1.33) in patients with normal renal

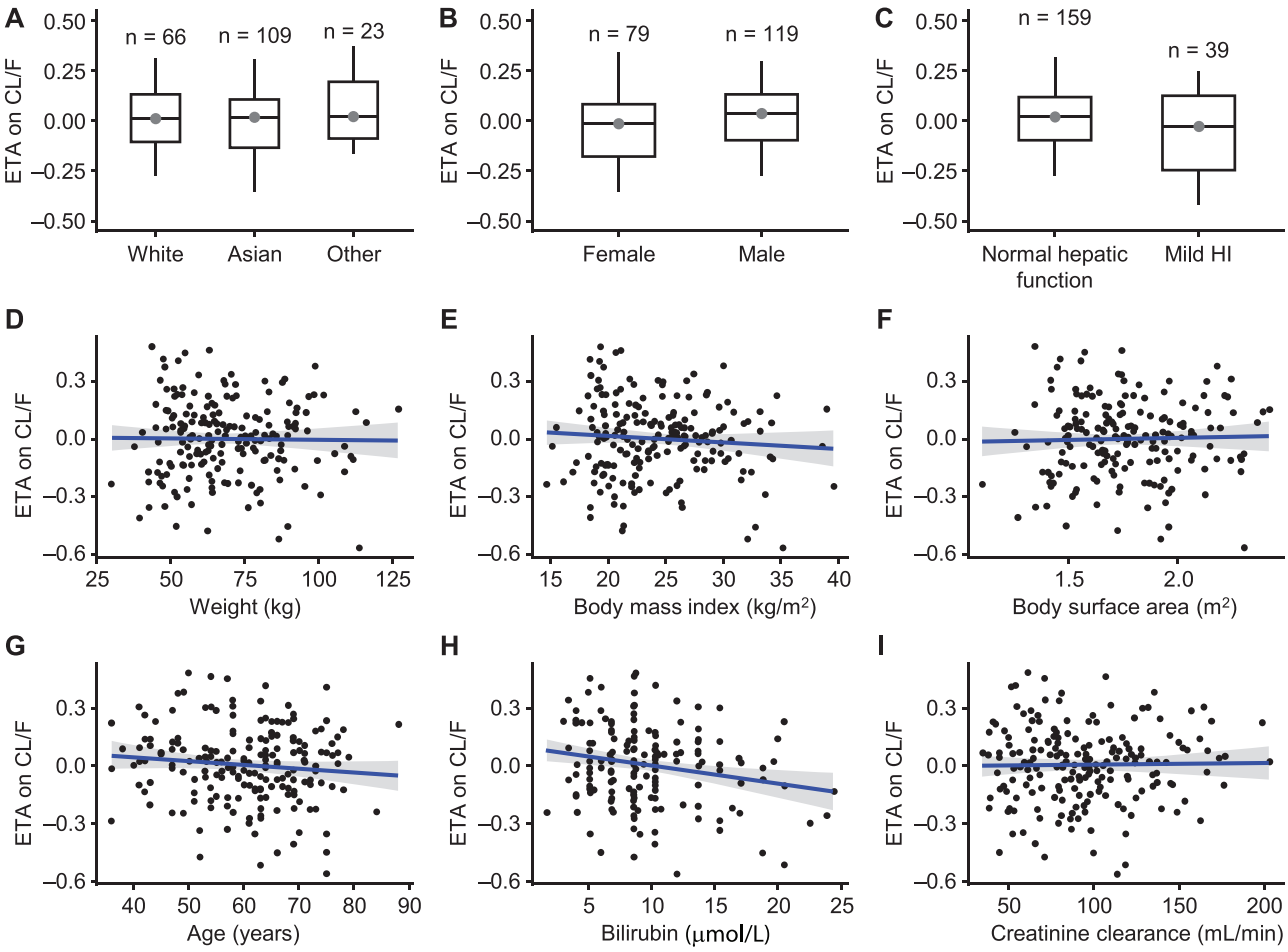

Figure 2. Relationship between covariates and individual random effects (ETA) on TAK-931 CL/F. Panels A–C box plots: horizontal lines comprising the box are the 25th, 50th (median), and 75th percentiles. The whisker ends denote 1.5 times the difference between the 25th and 75th percentiles. Panels D–I: black closed circles are the individual ETA on apparent clearance; the blue lines show linear regressions, and gray shades are corresponding 95% confidence intervals of linear regressions. CL/F, apparent oral clearance; ETA, empirical Bayes estimate of the interindividual random effect; HI, hepatic impairment.

function, mild renal impairment, and moderate renal impairment, respectively. A substantial overlap was observed in the 5th and 95th percentiles of normalized AUC, which were obtained in each renal function category of the typical study. The impact of body weight was investigated in 3 categories of body weight corresponding to the observed body weight tertiles of the population (low, 37.5-62.6 kg; medium, >62.6-79.2 kg; high, >79.2-127 kg). The median normalized AUC (90%CI, reflecting parameter uncertainty) was 0.803 (0.749-0.873), 0.959 (0.949-0.967), and 1.14 (1.08-1.19) in patients with low, medium, and high body weights, respectively. A large overlap was observed in the 5th and 95th percentiles of normalized AUC, which were obtained in each body weight tertile of the typical study. Accordingly, dose adjustments based on body weight and/or mild to moderate renal impairment was not warranted. The effects of other factors on TAK-931 exposures during covariate analysis are illustrated in Figure S5.

Discussion

Model-informed approaches are vital to the success of accelerated oncology drug development programs.[29,30] A population PK model was developed for TAK-931 using pooled plasma concentration data obtained from 198 patients in 3 phase 1 and phase 2 studies. A 2-compartment model with 2 transit compartments describing the absorption and first-order linear elimination adequately characterized the PK of TAK-931. The model included random effects (η) to quantify the unexplained IIV in CL/F and MTT. Including a random effect on V_c/F did not result in a statistically significant improvement of the model fit. This was presumably due to the larger amount of data available around the

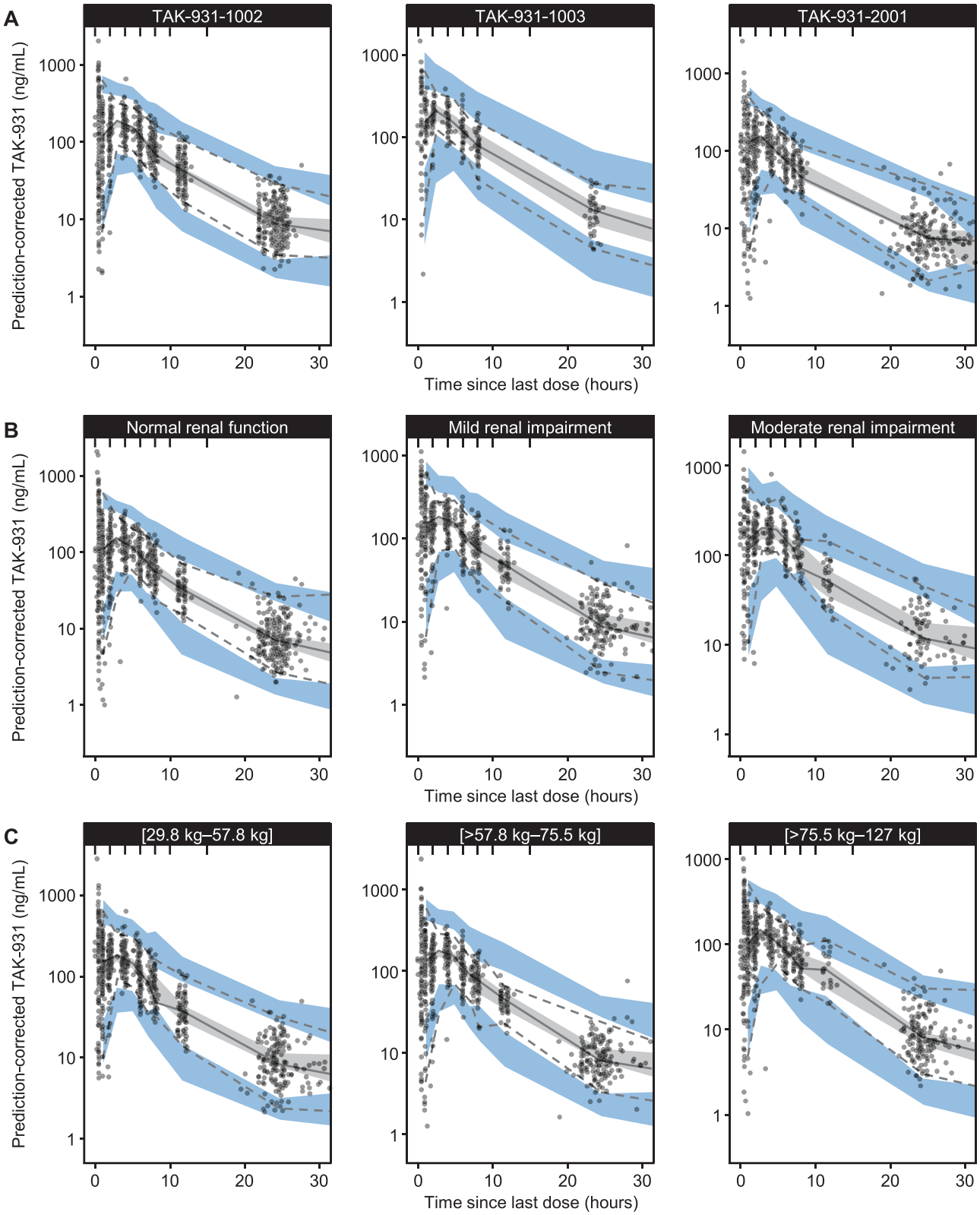

Figure 3. Prediction-corrected visual predictive check of the final population pharmacokinetic model stratified by study (A), renal status (B), and body weight tertiles (C) during the first 30 hours postdose. Open gray circles are individual data points. The solid black line is the median of the observed data, and the dashed black lines are the 2.5th and 97.5th percentiles of the observed data. The gray shaded area is the 95% confidence interval of the simulated median, and the lighter blue shaded areas are the 95% confidence intervals of the simulated 2.5th and 97.5th percentiles of the simulated data. Moderate renal impairment, 30 mL/min $\leq$ CrCL $<$ 60 mL/min; mild renal impairment, 60 mL/min $\leq$ CrCL $<$ 90 mL/min; and normal renal function, 90 mL/min $\leq$ CrCL. CrCL, creatinine clearance.

Table 3. Final Model Parameter Estimates and Bootstrap Results for the Final Model

	Final Model			Bootstrap Analysis	
	Estimate	RSE (%)	Shrinkage (%)	Median	95%CI
CL/F, L/h	38.0	0.6	…	38.0	36.1-39.7
V_c/F, L	194	0.5	…	194	185-204
Q/F, L/h	7.71	2.4	…	7.73	7.00-8.56
V_p/F, L	140	1.6	…	140	120-164
MTT, h	0.756	17.3	…	0.760	0.688-0.831
Covariate exponent for creatinine clearance on CL/F	0.325	15	…	0.324	0.236-0.422
Covariate exponent for body weight on CL/F	0.484	21.8	…	0.479	0.272-0.674
Covariate exponent for body weight on V_c/F	0.867	11.4	…	0.858	0.670-1.06
Covariate exponent for body weight on Q/F	0.938	15.7	…	0.926	0.617-1.27
IIV on CL/F, %CV	22.7	6.9	13.4	22.5	19.2-25.6
IIV on MTT, %CV	65.6	5.8	10.3	65.1	56.8-74.8
Additive residual error (standard deviation) in log scale	0.499	4	6.3	0.500	0.462-0.542

CI, confidence interval; CL/F, apparent oral clearance; CV, coefficient of variation; IIV, interindividual variability; MTT, mean transit time; Q/F, apparent intercompartmental clearance; RSE, relative standard error; V_c/F, apparent central compartment volume; V_p/F, apparent peripheral compartment volume.
CV was obtained from the variance according to the following equation: $CV=\sqrt{(\exp(\omega^2)-1)}$. All data are presented to 3 significant digits, except RSE (%), which is rounded to 1 decimal place.

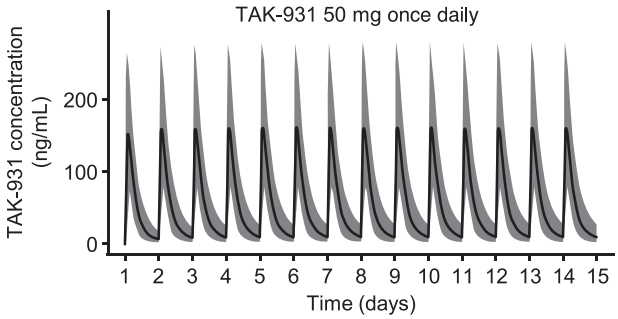

Figure 4. TAK-931 median (95% prediction interval) concentration-time profiles at 50 mg once daily for 14 days. The black solid lines are the median of simulated data and the gray shaded areas are 95% confidence intervals.

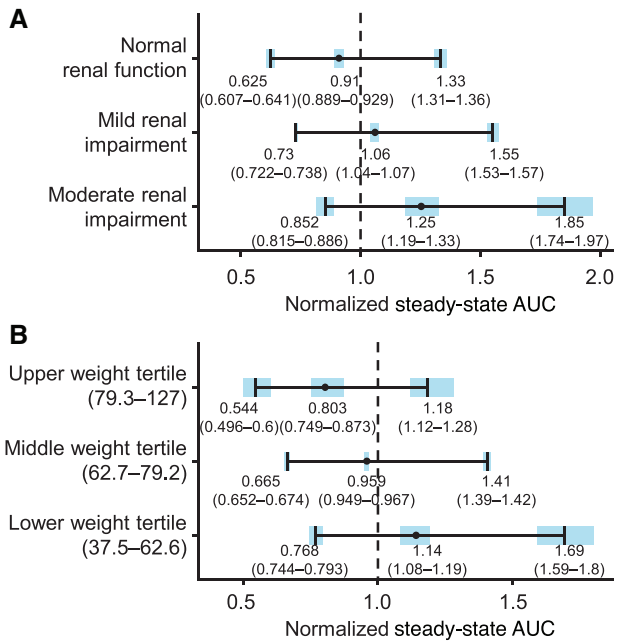

Figure 5. Forest plots of effect of renal function (normal, mild, or moderate renal impairment) and body weight on the steady-state exposure of TAK-931 following administration at 50 mg once daily. Black circles and associated horizontal error bars represent the median, 5th, and 95th percentiles of the normalized steady-state AUC (typical study educated by the final model parameters). Blue shaded areas represent the 90%CI of the model predictions. Normalized AUC was derived relative to the reference patient, with a CrCL of 90.45 mL/min and a body weight of 65.95 kg. Moderate renal impairment, 30 mL/min $\leq$ CrCL $<$ 60 mL/min; mild renal impairment, 60 mL/min $\leq$ CrCL $<$ 90 mL/min; and normal renal function, 90 mL/min $\leq$ CrCL $<$ 150 mL/min. Lower weight tertile, 37.5–62.6 kg; middle weight tertile, $>$62.7–79.2 kg; upper weight tertile, $>$79.3–127 kg. Reference patient CrCL, 90.45 mL/min; body weight, 65.95 kg. AUC, area under the plasma concentration–time curve; CI, confidence interval; CrCL, creatinine clearance.

absorption process compared to the disposition area that led to the significant inclusion of IIV on MTT instead of V_c/F. The random effect on CL/F and MTT was estimated with a good precision (relative standard error $<$7%), and the corresponding η-shrinkage values for CL/F and MTT were acceptable ($<$30%) in the base model without covariate relationships. The final model identified CrCL as a statistically significant ($P < .001$) covariate of CL/F and body weight as a statistically significant covariate ($P < .001$) of CL/F, V_c/F, and Q/F.

TAK-931 demonstrated pH-dependent solubility and freely soluble below pH 5. Gastric pH-modifying agents were excluded from the clinical studies. It has high permeability and is not a substrate for P-glycoprotein on the basis of transcellular transport investigations across Caco-2 cell monolayers. Investigations into cytochrome P450 (CYP) enzyme-mediated metabolism showed that CYP2D6 and

CYP3A4/5 are the main CYPs involved in the metabolism of TAK 931. Subsequent investigations into uridine diphosphate-glucuronosyltransferase (UGT)-mediated metabolism showed that UGT1A9 is the primary UGT involved in the metabolism of TAK 931, followed by UGT1A1, 1A4, and 1A7. The drug–drug interaction potential with CYP inhibitors is unlikely; however, there is a drug–drug interaction potential with metabolic enzyme inducers. Therefore, strong metabolic enzyme inducers (eg, rifampin) were excluded during the study treatment. TAK-931 was administered to patients on an empty stomach except water from 2 hours before taking the study drug until 4 hours after dosing. In addition, a dedicated relative bioavailability study (NCT03708211) demonstrated that capsule and tablet were bioequivalent (Takeda, data on file); therefore, the effect of formulation on TAK-931 PK was not assessed during the covariate model development. Among 80 patients with various advanced solid tumors enrolled in the TAK-931 phase 1 dose escalation study (NCT02699749), the most common disease type at diagnosis was esophageal cancer (16%), followed by pancreatic cancer (13%), and cervical and rectal cancer (5% each). Based on TAK-931 PK characterized by the noncompartmental analysis, tumor types had no impact on the PK of TAK-931. A recommended phase 2 dose of 50 mg once daily for 14 days in a 21-day treatment cycle was determined in the patient population of advanced solid tumors.

The simulated exposure after once-daily administration of 50 mg TAK-931 during 14 days showed a rapid attainment of the steady state of TAK-931 exposures after 3 days of treatment, consistent with the estimated half-life of 6 hours. Overall, the median exposure of TAK-931 increased by 18% between days 1 and 14, indicating minimum drug accumulations following multiple-dose administration.

The impact of the body weight and renal function on steady-state exposures of TAK-931 was assessed. Comparing to patients with normal renal function, the median normalized TAK-931 steady-state AUC values obtained in patients with mild or moderate renal impairment were within 0.80 to 1.25, suggesting that dose adjustment was not necessary in patients with mild to moderate renal impairment. Although there was a trend for higher TAK-931 exposures with lower CrCL, the distributions of individual predicted exposures substantially overlapped among the renal function categories. Urine TAK-931 PK data were obtained from 79 patients in the phase 1 dose finding study (NCT02699749). Based on the estimated amount of TAK-931 excreted in urine, the renal clearance of TAK-931 was ≈8% of TAK-931 total apparent clearance, indicating that renal clearance was not a major clearance pathway for overall TAK-931 clearance. This is consistent with the conclusion that no dose adjustment is needed for patients with mild or moderate renal impairment. Similarly, the median normalized AUC obtained in the 3 body weight groups were within 0.80 to 1.25 in comparison with a typical patient. The trend of higher TAK-931 exposures was observed with lower body weights. Considering the overall variability of the estimated normalized TAK-931 AUC and substantial overlap of TAK-931 steady-state exposures among these body weight groups, body weight had no clinically meaningful impact on TAK-931 CL/F. The interaction of impact of body weight and renal function was explored. Simulations that accounted for the correlation between weight and CrCL suggested an ≈50% increase in TAK-931 steady-state exposures for patients with low body weight and poor renal function (Figure S6). The most common treatment-emergent adverse events (occurring in ≥20% of patients) in the phase 2 study (TAK-931-2001) were nausea (47.5%), vomiting (35.6%), decreased appetite (33.7%), decreased neutrophil count (26.7%), fatigue (23.8%), and abdominal pain (20.8%). These adverse events can be monitored and managed through protocol-specified dose modification guidance. Due to limited safety data available for patients with low body weight and poor renal function, these patients should be closely monitored for toxicities.

The first-in-human clinical study of TAK-931 was conducted in Japan. A recommended phase 2 dose of 50 mg once daily for 14 days in a 21-day treatment cycle was selected. This dosing schedule was further evaluated in a Western patient population in the phase 2 study. A safety lead-in cohort was included in the phase 2 study to confirm the comparable TAK-931 systemic exposures and safety profiles between Japanese and Western patients. In this population analysis, race was not identified as a statistically significant covariate on TAK-931 CL/F. The comparable CL/F across races (Figure 1A) supports the same starting dose of TAK-931 in the global patient populations. In addition, sex, age (36-88 years), and mild hepatic impairment had no impact on TAK-931 CL/F, indicating no need of dose adjustment for these patient-specific factors.

Conclusions

A population PK analysis was performed to characterize sources of variability on the PK of TAK-931 in 198 adult patients with advanced solid tumors. A 2-compartment model with 2 transit compartments adequately described the PK of TAK-931. Race (Asian vs Western), sex, age (36-88 years), Eastern Cooperative Oncology Group status (0 or 1), body weight (29.8-127 kg), mild hepatic impairment, and mild to moderate renal impairment (CrCL ≥35 mL/min) had no clinically

meaningful impact on TAK-931 PK. The analysis supports the same starting dose of TAK-931 in adult patients with cancer in a global setting.

Acknowledgments

The authors thank the patients and their families and caregivers for their participation in the studies used for this analysis, along with all investigators and site personnel. The authors were assisted in the preparation of the manuscript by Flowers Lovern, a professional Medical Writer contracted to Medical Writing Innovations (Raleigh, North Carolina). This assistance was funded by Millennium Pharmaceuticals, Inc., Cambridge, Massachusetts, a wholly owned subsidiary of Takeda Pharmaceutical Company Limited.

Conflicts of Interest

N.G. and X.Z. are current employees of Millennium Pharmaceuticals, Inc., Cambridge, Massachusetts, a wholly owned subsidiary of Takeda Pharmaceutical Company Limited. A.O. and P.M.D. are employees of Certara, Data Science Services, which was compensated by Takeda for the analyses performed.

Funding

Funding for this research was provided by Millennium Pharmaceuticals, Inc., Cambridge, Massachusetts, a wholly owned subsidiary of Takeda Pharmaceutical Company Limited.

Data-Sharing Statement

The datasets, including the redacted study protocol, redacted statistical analysis plan, and individual participants data supporting the results reported in this article, will be made available within three months from initial request, to researchers who provide a methodologically sound proposal. The data will be provided after its de-identification, in compliance with applicable privacy laws, data protection, and requirements for consent and anonymization.

References

1. Bonte D, Lindvall C, Liu H, Dykema K, Furge K, Weinreich M. Cdc7-Dbf4 kinase overexpression in multiple cancers and tumor cell lines is correlated with p53 inactivation. *Neoplasia*. 2008;10(9):920-931.
2. Montagnoli A, Moll J, Colotta F. Targeting cell division cycle 7 kinase: a new approach for cancer therapy. *Clin Cancer Res*. 2010;16(18):4503-4508.
3. Hou Y, Wang HQ, Ba Y. High expression of cell division cycle 7 protein correlates with poor prognosis in patients with diffuse large B-cell lymphoma. *Med Oncol*. 2012;29(5):3498-3503.
4. Kulkarni AA, Kingsbury SR, Tudzarova S, et al. CDC7 kinase is a predictor of survival and a novel therapeutic target in epithelial ovarian carcinoma. *Clin Cancer Res*. 2009;15(7):2417-2425.
5. Melling N, Muth J, Simon R, et al. CDC7 overexpression is an independent prognostic marker and a potential therapeutic target in colorectal cancer. *Diagn Pathol*. 2015;10:125.
6. Abraham RT. Cell cycle checkpoint signaling through the ATM and ATR kinases. *Genes Dev*. 2001;15(17):2177-2196.
7. Cheng AN, Jiang SS, Fan CC, et al. Increased CDC7 expression is a marker of oral squamous cell carcinoma and overexpression of CDC7 contributes to the resistance to DNA-damaging agents. *Cancer Lett*. 2013;337(2):218-225.
8. Labib K. How do CDC7 and cyclin-dependent kinases trigger the initiation of chromosome replication in eukaryotic cells? *Genes Dev*. 2010;24(12):1208-1219.
9. Masai H, Arai K. CDC7 kinase complex: a key regulator in the initiation of DNA replication. *J Cell Physiol*. 2002;190(3):287-296.
10. Yamada M, Masai H, Bartek J. Regulation and roles of CDC7 kinase under replication stress. *Cell Cycle*. 2014;13(12):1859-1866.
11. Huggett MT, Tudzarova S, Proctor I, et al. CDC7 is a potent anti-cancer target in pancreatic cancer due to abrogation of the DNA origin activation checkpoint. *Oncotarget*. 2016;7(14):18495-18507.
12. Kurasawa O, Miyazaki T, Homma M, et al. Discovery of a novel, highly potent, and selective thieno[3,2-d]pyrimidinone-based Cdc7 inhibitor with a quinuclidine moiety (TAK-931) as an orally active investigational antitumor agent. *J Med Chem*. 2020;63(3):1084-1104.
13. NIH US National Library of Medicine. A study to evaluate TAK-931 in participants with advanced nonhematologic tumors. https://clinicaltrials.gov/ct2/show/NCT02699749. Accessed July 19, 2021.
14. NIH US National Library of Medicine. A study to assess the relative bioavailability, effect of food, and gastric potential hydrogen (pH) modification on the pharmacokinetics (PK) of TAK-931 in participants with advanced solid tumors. https://clinicaltrials.gov/ct2/show/NCT03708211. Accessed July 19, 2021.
15. NIH US National Library of Medicine. A study to evaluate the safety, tolerability, and activity of TAK-931 in participants with metastatic pancreatic cancer, metastatic colorectal cancer, and other advanced solid tumors. https://www.clinicaltrials.gov/ct2/show/NCT03261947. Accessed July 19, 2021.
16. Shimizu T, Doi T, Kondo S, et al. First-in-human phase 1 study of TAK-931, an oral cell division cycle 7 (CDC7) inhibitor, in patients (pts) with advanced solid tumors. *J Clin Oncol*. 2018;36(15 suppl):2506-2506.
17. US Food and Drug Administration. Guidance for industry: E6(R2) good clinical practice: integrated addendum to ICH E6(R1). https://www.fda.gov/files/drugs/published/E6%28R2%29-Good-Clinical-Practice–Integrated-Addendum-to-ICH-E6%28R1%29.pdf. Accessed July 19, 2021.
18. Mould DR, Upton RN. Basic concepts in population modeling, simulation, and model-based drug development–part 2: introduction to pharmacokinetic modeling methods. *CPT Pharmacometrics Syst Pharmacol*. 2013;2:e38.
19. Jonsson EN, Karlsson MO. Automated covariate model building within NONMEM. *Pharm Res*. 1998;15(9):1463-1468.
20. Cockcroft DW, Gault MH. Prediction of creatinine clearance from serum creatinine. *Nephron*. 1976;16(1):31-41.
21. Gupta N, Diderichsen PM, Hanley MJ, et al. Population pharmacokinetic analysis of ixazomib, an oral proteasome inhibitor, including data from the phase III TOURMALINE-MM1 study to inform labelling. *Clin Pharmacokinet*. 2017;56(11):1355-1368.
22. Gupta N, Wang X, Offman E, et al. Population pharmacokinetics of brigatinib in healthy volunteers and patients with cancer. *Clin Pharmacokinet*. 2021;60(2):235-247.
23. Nguyen TH, Mouksassi MS, Holford N, et al. Model evaluation of continuous data pharmacometric models: metrics and graphics. *CPT Pharmacometrics Syst Pharmacol*. 2017;6(2):87-109.

24. Karlsson MO, Savic RM. Diagnosing model diagnostics. *Clin Pharmacol Ther*. 2007;82(1):17-20.
25. Yafune A, Ishiguro M. Bootstrap approach for constructing confidence intervals for population pharmacokinetic parameters. I: a use of bootstrap standard error. *Stat Med*. 1999;18(5):581-599.
26. Karlsson MO, Holford N. A tutorial on visual predictive checks [abstract]. www.page-meeting.org/?abstract=1434. www.page-meeting.org/?abstract=1434. Accessed July 19, 2021.
27. Bergstrand M, Hooker AC, Wallin JE, Karlsson MO. Prediction-corrected visual predictive checks for diagnosing nonlinear mixed-effects models. *AAPS J*. 2011;13(2):143-151.
28. Savic RM, Jonker DM, Kerbusch T, Karlsson MO. Implementation of a transit compartment model for describing drug absorption in pharmacokinetic studies. *J Pharmacokinet Pharmacodyn*. 2007;34(5):711-726.
29. Faucette S, Wagh S, Trivedi A, Venkatakrishnan K, Gupta N. Reverse translation of US Food and Drug Administration reviews of oncology new molecular entities approved in 2011–2017: lessons learned for anticancer drug development. *Clin Transl Sci*. 2018;11(2):123-146.
30. Gupta N, Hanley MJ, Diderichsen PM, et al. Model-informed drug development for ixazomib, an oral proteasome inhibitor. *Clin Pharmacol Ther*. 2019;105(2):376-387.

Supplemental Information

Additional supplemental information can be found by clicking the Supplements link in the PDF toolbar or the Supplemental Information section at the end of web-based version of this article.